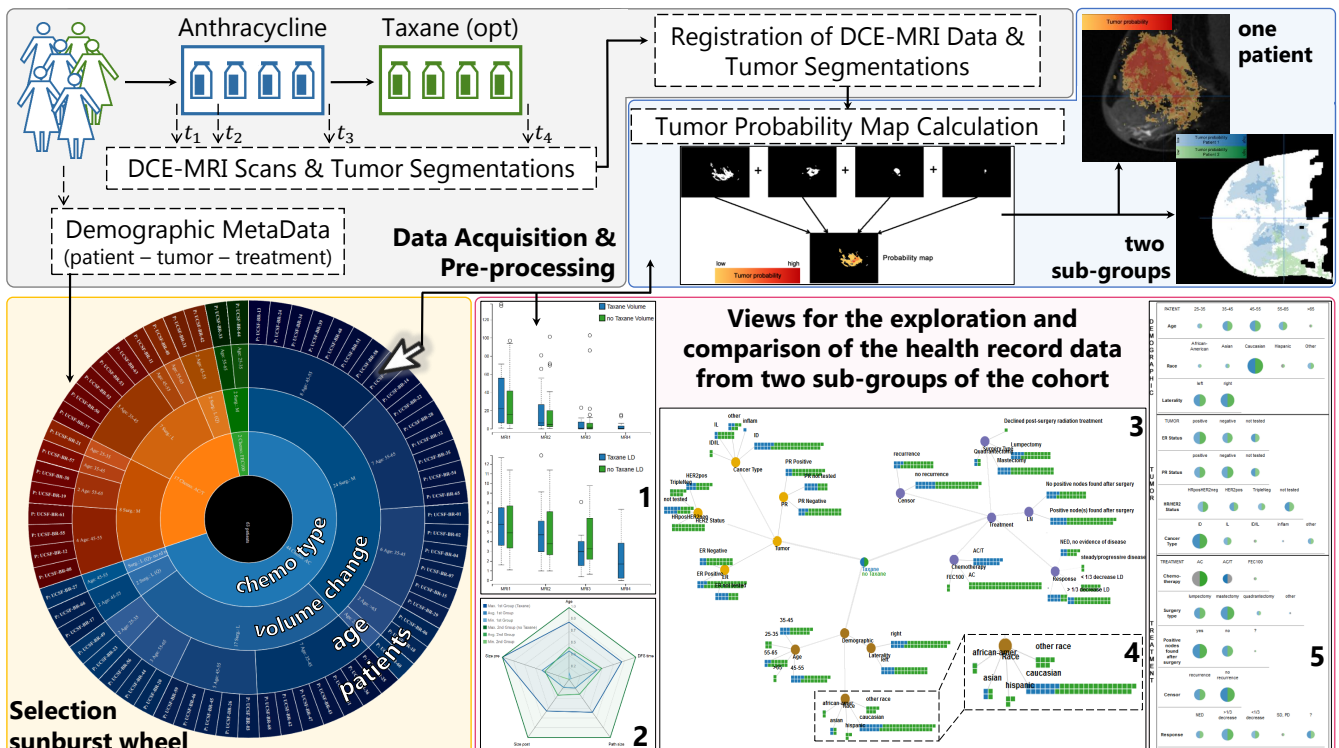# ChemoExplorer: A Dashboard for the Visual Analysis of Chemotherapy Response in Breast Cancer Patients

N. Karall[1], M.E. Gröller[1,2], R.G. Raidou[1]

[1]TU Wien, Austria, [2]VRVis Research Center, Austria

Figure 1: *Workflow of our proposed ChemoExplorer dashboard. After data acquisition and pre-processing (grey), a sunburst wheel (yellow) is employed to filter pairs of subjects (patients or groups) for comparison. From this selection, tumor control probability maps of the follow-up imaging data are created and visualized (blue). Finally, multiple linked visual representations (1-5) are employed to display different aspects of the non-imaging health record data of the patients (pink). For the latter, we illustrate here only the comparison of two groups.*

Abstract

In breast cancer chemotherapy treatment, different alternative strategies can be employed. Clinical researchers working on the optimization of chemotherapy strategies need to analyze the progress of the treatment and to understand how different groups of patients respond to selected therapies. This is a challenging task, because of the multitude of imaging and non-imaging health record data involved. We, hereby, introduce a web-based dashboard that facilitates the comparison and analysis of publicly available breast cancer chemotherapy response data, consisting of a follow-up study of 63 patients. Each patient received one of two available therapeutic strategies and their treatment response was documented. Our dashboard provides an initial basis for clinical researchers working on chemotherapy optimization, to analyze the progress of treatment and to compare the response of (groups of) patients with distinct treatment characteristics. Our approach consists of multiple linked representations that provide interactive views on different aspects of the available imaging and non-imaging data. To illustrate the functionality of the ChemoExplorer, we conducted a usage scenario that shows the initial results of our work.

CCS Concepts
●Human-centered computing → Visual analytics; ●Applied computing → Life and medical sciences;

delivered by
EUROGRAPHICS DIGITAL LIBRARY
www.eg.org   diglib.eg.org

1. Introduction

Breast cancer is the most common cancer among the female population [FSD*15]. As treatment, chemotherapy is often employed – alone, or together with other therapeutic procedures. Different combinations of chemotherapy drugs can be administered, and a lot of trials are taking place, with the goal of understanding the effect and suitability of alternatives for different patient groups.

For the purpose of this work, we employ a publicly available data set from a trial study of 63 breast cancer patients, undergoing chemotherapy [NH16]. A schematic depiction of the data acquisition procedure is shown in the grey panel of Figure 1. All 63 patients received chemotherapy treatment with *Anthracycline* in four cycles, administered every three weeks. A subset of 17 patients received an additional treatment with *Taxane*. Before treatment (t_1), the patients were scanned and *Dynamic Contrast Enhanced Magnetic Resonance Imaging (DCE-MRI)* data were acquired. DCE-MRI data are 4D data, i.e., MRI volumes showing the perfusion of tumors due to contrast agent absorption, across time [Tur09]. These scans were repeated after the first Anthracycline treatment (t_2), after the completion of all four Anthracycline cycles (t_3) and – if applicable – after the additional Taxane cycle (t_4). This data set contains also rough tumor segmentations for each patient at each treatment time point, as well as a multitude of *non-imaging* data. As non-imaging data we define health record data, containing the characteristics of the patients (e.g., age, race), the tumors (e.g., volume, diameter) and the treatment (e.g., type of treatment, response).

Clinical researchers working on trial studies for chemotherapy, such as the one mentioned above, need to analyze the progress of the patients during and after treatment, and to understand how different sub-groups of patients respond. Currently, this is a challenging task because of the multitude of patients, the multitude of follow-up time data and the availability of additional non-imaging data. Combining imaging data with electronic health records is a relatively new and challenging topic, and adequate visualization strategies to explore and analyze all available data are required.

The *contribution* of our work is the design of a web-based dashboard – the ChemoExplorer – for the detailed comparison and analysis of the progress of chemotherapy alternatives, within a group of patients. Our dashboard facilitates the *comparison and analysis of a multitude of imaging and non-imaging patient data*, such as the previously described ones. Our aim is to provide an initial conceptual basis, which can be later elaborated and generalized to cover also larger groups of patients, where more complex data comparison and analysis can be conducted.

2. Related Work

Previous work in the field of *tumor visualization* includes the MammoExplorer by Coto et al. [CGB*05], which combines advanced interaction, segmentation and visualization approaches for breast tumors. Rieder et al. [RWS*10] introduced an approach for displaying liver tumor surfaces using 2D maps. In *perfusion visualization*, Preim et al. [POM*09] give a comprehensive overview of basic and more advanced visualization techniques for the visualization of perfusion data. More recent work was conducted by Raidou et al. [RBV*14] with the introduction of an interactive tool to visually explore and analyze DCE-MRI data and their variability. Also,

Glasser et al. [GPTP10] addressed visual analytics approaches for breast cancer diagnosis and classification. Additionally, Raidou et al. [RCMM*16] proposed a visual analytics approach for analyzing alternative strategies in prostate cancer radiotherapy treatment.

In *comparative visualization*, Kim et al. [KCK17] presented a survey of strategies for comparing 3D and 4D data, providing a categorized overview on all previously proposed approaches. Last but not least, Steenwijk et al. [SMB*10] introduced a framework for the pre-processing and visualization of both imaging and non-imaging cohort data. A way to visually explore and analyze heterogeneous data in a cohort of patients was also described by Angelelli et al. [AOH*14], while Stolte et al. [STH02] proposed a framework to visualize data from large multidimensional databases. Closer to our approach is the work of Klemm et al. [KLR*13, KOJL*14]. Other approaches were recently proposed by Alemzadeh et al. [ANI*17] and Bannach et al. [BBJ*17].

Our work shares some aspects with several previous works. However, to the best of our knowledge, designing a simple dashboard that enables the detailed comparison and analysis of a multitude of data from follow-up studies and treatment response, has not been addressed. Our dashboard is an initial step for the visual comparison and analysis of patients throughout the entire treatment, incorporating both imaging and health record data.

3. The ChemoExplorer Dashboard

The scope of the ChemoExplorer is to provide a basis for clinical researchers, to compare and analyze both imaging and non-imaging data from the available treatment response data set. Our approach is schematically depicted in Figure 1.

After data acquisition (described in Section 1), a *pre-processing step* is performed. This involves registration [Bro92] and filtering, to render the imaging data from different patients comparable. We employ an affine transformation with a nearest neighbor interpolation, to register the available DCE-MRI scans of all patients at all treatment time points. The deformation field is then used to adapt the provided tumor segmentations. Deformation during the registration process brings uncertainty into the analysis [SFJ*16], but this was considered out of scope for the present work.

The dashboard initializes with an interface for the selection of criteria for the analysis and comparison of the patients, such as age of patients, laterality of tumor, chemotherapy type, etc. After this filtering, an interactive *sunburst representation* [SZ00] is created dynamically, to provide a visual overview on the available patient data, as shown in the yellow panel of Figure 1. The center of the sunburst represents the total cohort. The different rings display the filtering criteria, in order of filtering. These can be re-ordered, to adapt interactively the sunburst. The outer ring corresponds to the individual patients. At this point, the expert can select subjects to analyze and compare. As *subjects* we denote individual patients, pairs of patients, or pairs of patient sub-groups. We limit the comparison to two subjects, as we are specifically interested in the comparison of the two available treatment strategies. For a more generalized application, the proposed visualization should be adapted, as it could face scalability issues for a higher number of patients, and for a higher number of comparisons.

After subject (one patient, two patients or two sub-groups) selection, the respective imaging and non-imaging follow-up data need to be analyzed. For the **imaging space**, the clinical researcher has to study the progress of the treatment and the shrinkage – or in some cases, increase – of the tumor, across time. To this end, the calculation and visualization of a *tumor probability map* was considered suitable, being a commonly employed concept in clinical practice [HBG02]. A tumor probability map is calculated from the registered binary masks of the segmented tumor data and indicates the locations of the breast that are more prone to tumor formation. This map is then overlaid on the initial imaging data (for the individual patient analysis) or a standardized breast (for more than one patient), as shown in the blue panel of Figure 1. For an individual patient, the colormap employed for the tumor probability is the heated-body scheme [LH92] with truncated ends, to avoid interference with the underlying greyscale values of the imaging data. For two patients or sub-groups, we use two sequential single-hue colormaps [HB03]. For the comparison of two subjects, both juxtaposition and superimposition are possible. However, for more than two subjects, this choice would need to be adapted [KCK17].

Multiple linked representations are employed for the **non-imaging data**, to enable experts to analyze and generate hypotheses, with respect to their medical health record data. Initially, we display the quantitative progress of a tumor volume and diameter in a simple *bar chart* representation, as shown in Figure 4 (bottom left). With this view, the intended expert can recognize the growth or decrease in the tumor volume or diameter through time. The horizontal axis is mapped to the four treatment time points (t_1-t_4). The upper vertical axis is mapped to the volume, and the lower to the diameter values, to save screen space. When comparing two patients, the bar charts are shown side-by-side at each time point, using different hues. For two sub-groups, the bar charts are substituted with *box plots* to show the entire distribution of values, as shown in the pink panel of Figure 1(1). For the volume and diameter, we use colors differing in saturation, as the hue is used consistently in the pairwise comparison, to denote different patients or sub-groups.

The selected non-imaging data can be compared also in *radar charts* [Cha18]. These are known iconographic representations that enable to discern shape differences. An example is depicted in the pink panel of Figure 1(2). Here, we depict the range within which the selected values are found – i.e., the minimum and maximum value – with high transparency, for visibility reasons. The two subjects are denoted with distinct colors, following the same color scheme as in the bar charts or box plots. For individual patients, this radar chart is simplified to polylines.

To show the division of the non-imaging data, we adopt an undirected rooted tree metaphor. This provides a structured, hierarchical data arrangement. Our *health record tree* is depicted in the pink panel of Figure 1(3). The root represents the entire cohort and its first-level vertices are the three non-imaging data categories (patient data, tumor data, treatment data). To these categories, we assign different colors [HB03]. The children of these three vertices encode different data variables. For individual patient analysis, these can be shown as simple nodes, with labels carrying the respective data values. For pairwise comparison of two patients, the nodes are split into two parts. If the values of the two patients are
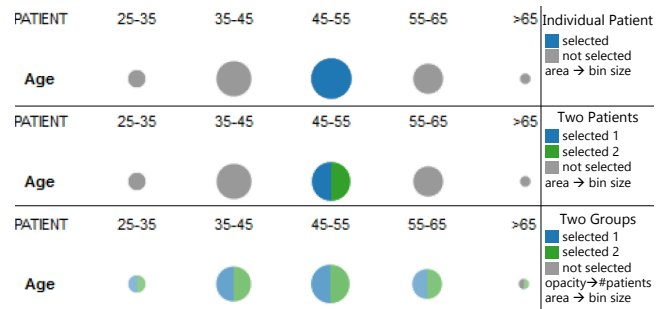
Figure 2: *The encodings employed in the spot matrix (from top to bottom: individual patient, two patients, two groups of patients).*

different, then the values are encoded to each node part. Otherwise, the node is not split, to reduce visual clutter in the tree. Finally, if two sub-groups are being explored and compared, the nodes are substituted by *waffle charts*, as presented in Figure 1(4). Waffle charts encode the distribution of the non-imaging data, belonging to each group, to a number of small colored squares. Distinct hues correspond to the two distinct groups. This design is expected to facilitate discerning differences, especially if the data have a hierarchical structure with a lot of subcategories.

An alternative to the health record tree is the *spot matrix*, presented in the pink panel of Figure 1(5). This view encodes the quantities of patients, falling within certain values of all non-imaging data subcategories. The quantity of each variable is mapped to the area of circular glyphs and the specific subject selection is highlighted. For one patient, highlighting is done through color encoding. For two patients, we follow the same approach as in the tree. We split the glyph into two parts (one for each patient) and we highlight the respective part through hue encoding. For group comparison, node splitting and hue encoding is followed by an additional opacity mapping, to depict the number of patients falling within a specific bin of values of a data variable. An example of this encoding is shown in Figure 2. An alternative to the spot matrix would be to use linked histograms, but the former was preferred as the glyph-like representation may provide easier and faster distinction, especially with an increasing number of attributes.

Implementation — The dashboard was implemented in Javascript, using Papaya for the visualization of imaging data, and D3.js for the information visualization plots. To handle the available non-imaging data, a MySQL database was built, which can be accessed by the dashboard in real time with PHP. The pre-processing was performed in MeVisLab.

4. Results

In this section, we present initial results that can be achieved with the use of our proof-of-concept dashboard. We begin the analysis by selecting a number of criteria for the creation of the sunburst wheel. Age of the patient, tumor volume change and type of chemotherapy (Anthracycline A, or Anthracycline/Taxane A/T) are selected. The sunburst wheel, shown in the yellow panel of Figure 1, is rendered and allows to select subjects for further analysis and comparison. Due to the page limit, we illustrate only two scenarios for the comparison of two subjects from the cohort: one

for the comparison of *two patient groups* receiving different treatments, and one for *two patients* from different age division.

Comparison of different chemotherapy treatment strategies — For this scenario, we select the two sub-groups that received one of two different chemotherapy strategies (Anthracycline `A`, or Anthracycline/Taxane `A/T`). When looking at the juxtaposed comparison of the tumor visualization maps (Figure 3), it can be seen that the distribution of the tumor probability in the `A/T` group (left) is different than in the `A` group (right). The tumor probability map of the latter is more disperse. This could be due to the size of the group, which might be resulting in a higher variability. The box plots in Figure 1(1) show that the average of the tumor volume and diameter have decreased through treatment time, for both groups. As only patients undergoing `A/T` chemotherapy were scheduled for a fourth DCE-MRI scan, no data is available for t_4 in the `A` group. Also, in the `A/T` group (blue), the tumor volume and diameter after t_3 decreased more than in the `A` group (green).

The radar chart in Figure 1(2) shows large variability in all explored data for both groups (age, DFS time, path size, size pre-surgery, size post-surgery). This can be seen in the large difference between the maximum and minimum values. When comparing the respective average values, we see that the drop of tumor size in the `A/T` group (blue) is bigger than in the `A` group (green). This was also confirmed by the findings of the box plots. For all other variables, no significant difference can be seen. The spot matrix in Figure 1(5) demonstrates small differences in the non-imaging data. Almost all properties are represented by approximately the same percentage of patients within the group, as shown by the similar opacity of the circle segments. Finally, the tree of Figure 1(3) and its extended waffle charts (4) show in detail how many patients represent the various categories. For example, we can see that most of the patients are of caucasian race.

**Comparison of two patients from different age divisions** — For this scenario, we select two patients: one among the youngest (25-35 years) and one among the oldest (>65) age division. Both patients did not receive Taxane and showed a tumor volume drop larger than 70%, as seen in the sunburst wheel. The tumor probability maps of these two patients are shown superimposed in Figure 4. The bar chart in Figure 4 shows that both patients had about the same tumor volume at t_1. This was 40.72 cm^3 (cc) for the older patient (blue) and 43.05 cm^3 (cc) for the younger patient (green). The treatment of the younger patient is faster and more effective than

the older patient, because a large volume drop is seen at t_2. In the radar chart, the difference in the post-chemotherapy tumor size is obvious. Commonalities and differences between the two patients can be also identified in the spot matrix, in Figure 4. While these patients do not have anything in common concerning non-imaging data such as age, race or breast laterality, the tumor characteristics are the same. For example, both patients showed positive lymph nodes, after surgery.

5. Conclusions and Future Work

We introduced a conceptual approach for the comparison and analysis of chemotherapy treatment response data, consisting of both imaging and non-imaging data. Individual patient follow-up studies and comparative analysis of two patients or sub-groups are made possible with our approach. The conceptual idea of this work is based on the specific available data set, for which only pairwise comparisons and analysis are required. For the comparison of more than two subjects, it is required to adapt the employed visualizations. This would be particularly interesting, in combination with more automatized ways of sub-group identification and selection. Linking to prediction of the treatment outcome of new patients, based on similarities to existing patients, is another clinically relevant future direction. Finally, an evaluation is also required, to validate the usefulness of the proposed approach and to assess the suitability of our design choices. Our ChemoExplorer is a basis to further abstract the approach by incorporating other (also larger) data sets, to generalize the design of the employed visualizations and to consult experts, in the future.
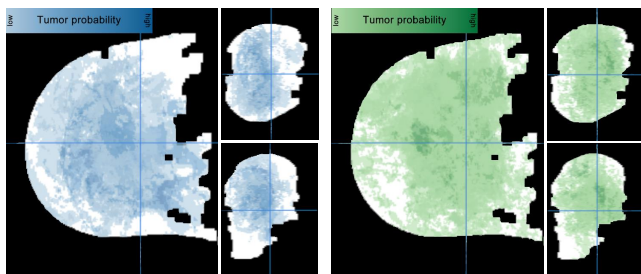
Figure 3: *Juxtaposed comparison of the tumor probability maps of the Anthracycline/Taxane (`A/T`) (left, blue) and the Anthracycline only (`A`) group (right, green) overlaid on a standardized breast (white mask), after registration. Superimposition is also possible.*
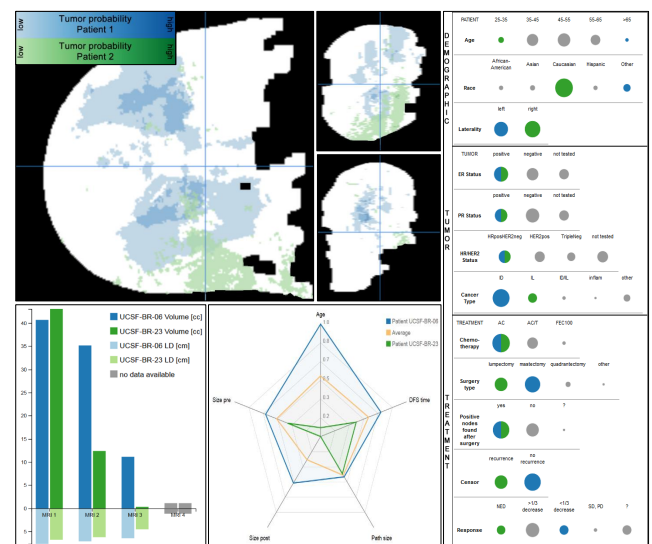
Figure 4: *Usage scenario for the visual comparison of two patients from different age groups (young patient: green, old patient: blue).*

References

[ANI*17] ALEMZADEH S., NIEMANN U., ITTERMANN T., VÖLZKE H., SCHNEIDER D., SPILIOPOULOU M., PREIM B.: Visual analytics of missing data in epidemiological cohort studies. In *Eurographics Workshop on Visual Computing for Biology and Medicine* (2017), vol. 4. 2

[AOH*14] ANGELELLI P., OELTZE S., HAÁSZ J., TURKAY C., HODNELAND E., LUNDERVOLD A., LUNDERVOLD A. J., PREIM B., HAUSER H.: Interactive visual analysis of heterogeneous cohort-study data. *IEEE Computer Graphics and Applications 34*, 5 (2014), 70–82. 2

[BBJ*17] BANNACH A., BERNARD J., JUNG F., KOHLHAMMER J., MAY T., SCHECKENBACH K., WESARG S.: Visual analytics for radiomics: Combining medical imaging with patient data for clinical research. In *Proceedings of the 2017 Workshop on Visual Analytics in Healthcare (VAHC)* (2017). 2

[Bro92] BROWN L. G.: A survey of image registration techniques. *ACM computing surveys (CSUR) 24*, 4 (1992), 325–376. 2

[CGB*05] COTO E., GRIMM S., BRUCKNER S., GRÖLLER M. E., KANITSAR A., RODRIGUEZ O.: MammoExplorer: An Advanced CAD Application for Breast DCE-MRI. In *Proceedings of Vision, Modelling, and Visualization 2005* (2005), pp. 91–98. 2

[Cha18] CHAMBERS J. M.: *Graphical methods for data analysis*. CRC Press, 2018. 3

[FSD*15] FERLAY J., SOERJOMATARAM I., DIKSHIT R., ESER S., MATHERS C., REBELO M., PARKIN D. M., FORMAN D., BRAY F.: Cancer incidence and mortality worldwide: sources, methods and major patterns in GLOBOCAN 2012. *International journal of cancer 136*, 5 (2015). 2

[GPTP10] GLASSER S., PREIM U., TÖNNIES K., PREIM B.: A visual analytics approach to diagnosis of breast DCE-MRI data. *Computers & Graphics 34*, 5 (2010), 602–611. 2

[HB03] HARROWER M., BREWER C. A.: Colorbrewer. org: an online tool for selecting colour schemes for maps. *The Cartographic Journal 40*, 1 (2003), 27–37. 3

[HBG02] HO S., BULLITT E., GERIG G.: Level-set evolution with region competition: automatic 3-D segmentation of brain tumors. In *Pattern Recognition, 2002. Proceedings. 16th International Conference on* (2002), vol. 1, IEEE, pp. 532–535. 3

[KCK17] KIM K., CARLIS J. V., KEEFE D. F.: Comparison techniques utilized in spatial 3D and 4D data visualizations: A survey and future directions. *Computers & Graphics 67* (2017), 138–147. 2, 3

[KLR*13] KLEMM P., LAWONN K., RAK M., PREIM B., TÖNNIES K. D., HEGENSCHEID K., VOLZKE H., OELTZE S.: Visualization and analysis of lumbar spine canal variability in cohort study data. In *VMV* (2013), pp. 121–128. 2

[KOJL*14] KLEMM P., OELTZE-JAFRA S., LAWONN K., HEGENSCHEID K., VOLZKE H., PREIM B.: Interactive visual analysis of image-centric cohort study data. *IEEE Transactions on Visualization and Computer Graphics 20*, 12 (2014), 1673–1682. 2

[LH92] LEVKOWITZ H., HERMAN G. T.: The design and evaluation of color scales for image data. *IEEE Computer Graphics and Applications 12*, 1 (1992), 72–80. 3

[NH16] NEWITT D., HYLTON N.: Single site breast DCE-MRI data and segmentations from patients undergoing neoadjuvant chemotherapy. In *The Cancer Imaging Archive* (2016). 2

[POM*09] PREIM B., OELTZE S., MLEJNEK M., GRÖLLER E., HENNEMUTH A., BEHRENS S.: Survey of the visual exploration and analysis of perfusion data. *IEEE Transactions on Visualization and Computer Graphics 15*, 2 (2009), 205–220. 2

[RBV*14] RAIDOU R. G., BREEUWER M., VILANOVA A., VAN DER HEIDE U. A., VAN HOUDT P.: The iCoCooN: Integration of Cobweb Charts with Parallel Coordinates for Visual Analysis of DCE-MRI Modeling Variations. In *Eurographics Workshop on Visual Computing for Biology and Medicine* (2014), pp. 11–20. 2

[RCMM*16] RAIDOU R. G., CASARES-MAGAZ O., MUREN L., VAN DER HEIDE U. A., RØRVIK J., BREEUWER M., VILANOVA A.: Visual analysis of tumor control models for prediction of radiotherapy response. In *Computer Graphics Forum* (2016), vol. 35, Wiley Online Library, pp. 231–240. 2

[RWS*10] RIEDER C., WEIHUSEN A., SCHUMANN C., ZIDOWITZ S., PEITGEN H.-O.: Visual support for interactive post-interventional assessment of radiofrequency ablation therapy. In *Computer Graphics Forum* (2010), vol. 29, Wiley Online Library, pp. 1093–1102. 2

[SFJ*16] SCHLACHTER M., FECHTER T., JURISIC M., SCHIMEK-JASCH T., OEHLKE O., ADEBAHR S., BIRKFELLNER W., NESTLE U., BÜHLER K.: Visualization of deformable image registration quality using local image dissimilarity. *IEEE Transactions on Medical Imaging 35*, 10 (2016), 2319–2328. 2

[SMB*10] STEENWIJK M. D., MILLES J., BUCHEM M., REIBER J., BOTHA C. P.: Integrated visual analysis for heterogeneous datasets in cohort studies. In *IEEE VisWeek Workshop on Visual Analytics in Health Care* (2010), vol. 3, p. 3. 2

[STH02] STOLTE C., TANG D., HANRAHAN P.: Polaris: A system for query, analysis, and visualization of multidimensional relational databases. *IEEE Transactions on Visualization and Computer Graphics 8*, 1 (2002), 52–65. 2

[SZ00] STASKO J., ZHANG E.: Focus+context display and navigation techniques for enhancing radial, space-filling hierarchy visualizations. In *Information Visualization, 2000. InfoVis 2000. IEEE Symposium on* (2000), IEEE, pp. 57–65. 2

[Tur09] TURNBULL L. W.: Dynamic contrast-enhanced MRI in the diagnosis and management of breast cancer. *NMR in Biomedicine 22*, 1 (2009), 28–39. 2